Computers & Graphics 32 (2008) 695–703

Contents lists available at ScienceDirect

Computers & Graphics

journal homepage: www.elsevier.com/locate/cag

Technical Section

Layered deformation of solid model using conformal mapping ☆

Zhongxuan Luo *, Junxiao Xue

Department of Applied Mathematics, Dalian University of Technology, Dalian 116024, China

ARTICLE INFO

Article history:
Received 9 November 2007
Received in revised form
11 August 2008
Accepted 25 September 2008

Keywords:
Deformation
Conformal mapping
Geometric modeling

ABSTRACT

In this paper, we present a solid model deformation method based on layered conformal mapping. For a solid model represented by base patch and height field, the shape of the model can be deformed by interactive means, such as changing the base patch by conformal mappings and adjusting the height field by a pre-defined function. In our method, the deformation is predictable and the transformation function of the deformation can be expressed analytically by Schwarz–Christoffel formula. To perform a deformation of a cylinder to a desired solid of rotation hierarchically, a generalized Schwarz–Christoffel formula is also introduced. Numerical examples show that the proposed method is convenient and efficient to deform solid models, especially to solids with genus zero.

1. Introduction

One of the most important operations in computer graphics and computer-aided design is object deformation. This operation allows easy creation of plain shaped objects from regular shapes like spheres, and allows the deformation of exiting objects [1].

The purpose of deformation is to satisfy the geometric requirements, but more importantly, the understanding of the mutual dependence and internal continuity before and after the deformation facilitates its further applications in mathematics and scientific computations such as in CAGD or moving mesh computation. In addition, in many applications it is important to preserve some geometric and topological properties under shape changes of the models. The best-known example is probably model editing: The overall shape follows the specified global deformation while the properties like, e.g., continuity, surface direction and genus number, are preserved.

In this paper, we introduce a solid model deformation method based on layered conformal mapping. For a solid model of a product structure, we represent it by base patch and height field, and then the shape of the model can be deformed by interactive means, such as changing the base patch by conformal mappings and adjusting the height field by a pre-defined function. To perform a deformation of a cylinder to a desired solid of rotation hierarchically, a generalized Schwarz–Christoffel formula is also introduced in this paper.

Our approach is free of tools and requires no pre-processing. As such, it allows users to immediately manipulate the model directly and easily compute the corresponding explicit expression of the transformation and conveniently get the relationship between an original and its deformed model. In addition, due to the properties of conformal mapping, the deformation satisfies the demands on preserving some geometric and topological properties and still allows for considerable shape changes.

Although there are some topological restrictions in our current work, the presented method can be conveniently applied to a solid model with genus zero as numerically validated in our experiments. The main contribution of our work is that a layered conformal deformation scheme is studied, which not only satisfies the shape changing requirements but also is easy to be analyzed the mutual relationship between before and after deformation.

The rest of the paper is organized as follows. We will first review some related work in Section 2, followed by a brief sketch of conformal mapping theory in Section 3. Then we present an overview of our method in Section 4. Section 5 discusses the base patch mapping. We analyze the properties of the proposed deformation method in Section 6. In Section 7, two simple algorithms and some numerical examples are given. We conclude the paper in Section 8.

2. Related work

There has been a considerable amount of work on model deformation in recent years. All the deformation methods independent of the representation of underlying objects can be divided into two classes according to whether they require a deformation tool or not [2].

☆ The project is supported by NNSFC (Nos. 10771028, 60533060), Program of New Century Excellent Fellowship of NECC, and is partially funded by a DoD fund (DAAD19-03-1-0375).

* Corresponding author.
E-mail address: luozx9609@vip.sina.com (Z. Luo).

0097-8493/$ - see front matter © 2008 Elsevier Ltd. All rights reserved.
doi:10.1016/j.cag.2008.09.010

Watt [3] developed the global and local non-tools deformation method proposed by Barr [4] to include intuitive tools in controlling deformation, where the concept of factor curve was introduced. Another kind of deformation method with free of tools introduced by Borrel and Bechmann [5] is a space deformation. A large range of deformation shapes such as arbitrary shaped bumps can be designed using this technique.

As for the class of deformation methods which employ some deformation tools, it essentially falls into three kinds. That is FFD [6–8] (free-form deformation), AxDf [9] (axial deformation) and PsDf [10] (parametric surface deformation). FFD introduced by Sederberg and Parry is one of the most versatile and powerful tools for representing and modeling flexible objects. FFD uses a Bézier parallelepiped lattice as a deformation tool. The lattice is defined by its control points. The objects embedded in the lattice are deformed by simply moving the control points. AxDf defines a deformation technique that make use of a 3D axis for deforming existing objects. More precisely, the AxDf accomplishes the deformation by adopting a parametric curve as the axis. The object is then attached to the axis and deformed accordingly when the shape of the curve is changed. The method called PsDf is a new FFD controlled by parametric surfaces. PsDf adopts two parametric surfaces, namely a shape surface and a height surface, as deformation tools. Objects to be deformed are embedded into the parametric domain of a shape surface through mapping function. Similar to that of both FFD and AxDf, while the shape of the two parametric surfaces are modified, the deformation will be passed to the object automatically.

Alternative methods for various kinds of model deformation rely on a relative representation [11–15], namely Laplacian coordinates. Ju et al. [16] developed a similar deformation method based on mean value coordinates. In Ju's method, the model is enclosed by a control mesh and each vertex v in the model is represented as an affine combination of some control mesh's vertices p_j, and deformation is achieved by adjusting the control mesh and propagating the change to the model. However, the mean value coordinates method lacks the interior locality and non-negativity properties. Pushkar et al. [17] generalized and improved Ju's method by introducing harmonic coordinates so that their method succeeds all the figures of the mean value coordinates method and makes up for shortcomings of Ju's method. Alexa [18] presented a survey of the mesh editing methods based on discrete Laplace and Poisson models.

Zayer et al. [19] constructed harmonic fields over a manifold and applied them to guide local deformations for surface editing and to establish correspondence for deformation transfer between reference and target shape. Similar to Zayer's method, Huang et al. [20] introduced a deformation method based on a modified barycentric interpolation technique. The central idea of Huang's method is to add a local transformation on each control vertex for interpolation, and then the local transformations can be optimized to minimize the first-order discontinuity.

Our approach avoids factoring the relative representation by directly applying the deformation to the original model. Hence, our approach provides a computational efficient and simple framework for model deformation, especially for a model with genus zero.

3. Conformal mapping theory

Conformal mapping uses complex function to transform 2D domains (Fig. 1). An analytic function $f(z)$ is conformal at any point where non-zero derivative exists [21]. The derivative of $f(z)$ exists at a point z if and only if the partial derivatives of u and v exist and obey the Cauchy–Riemann conditions:

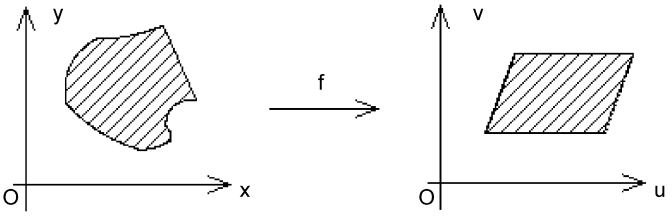

Fig. 1. Conformal mapping uses complex function to transform 2D domains.

$$\frac{\partial u}{\partial x}=\frac{\partial v}{\partial y} \quad \text{and} \quad \frac{\partial u}{\partial y}=-\frac{\partial v}{\partial x}, \tag{1}$$

where $z=x+\mathrm{i}y\in\mathscr{C}$, $f(z)=u+\mathrm{i}v\in\mathscr{C}$ and $\mathscr{C}$ is the complex field.

The existence of a conformal mapping between any two simply connected regions is guaranteed by the Riemann mapping theorem. The name of conformal mapping is derived from the properties by which it is characterized. To show these properties, consider an arc Γ given by $z(t)=x(t)+\mathrm{i}y(t)$, which lies in a domain D, where $t\in[a,b]$, $x(t),y(t)\in R$. Suppose $f(z)$ is analytic in D and the arc $f(\Gamma)$ is given by $w(t)=f(z(t))$. By the Chain rule, $w'(t)=f'(z(t))z'(t)$. It is obviously that $w'(t)\neq 0$ if $z'(t)\neq 0$ and $f'(z)\neq 0$, and furthermore,

$$arg(w')=arg(z')+arg(f'(z)) \quad \text{and} \quad |w'|=|f'(z)||z'|, \tag{2}$$

where arg is the argument of a complex number, and $|\cdot|$ is the modulus of a complex number. Eq. (2) can be geometrically interpreted as follows: The right angles between grid lines are preserved, and the stretching is uniform in all directions at any given point. Hence conformal mapping satisfies the local demands on rigidity and still allows for considerable global distortion [22].

4. Conformal mapping-based deformation

Let $V=(x_1,x_2,x_3)$ be a sampled point from a solid model P. In this paper, we focus on the solid models with manifolds as their constituent topological spaces and consider the model P to be restricted to the following so-called product structure.

Definition 1. If a solid model P is homeomorphic to the product $B\times F$, where $B=\{(x_1,x_2)|(x_1,x_2)\in R^2\}$ and $F=\{x_3|x_3\in R\}$, then we say that P is of a product structure.

Actually, a solid model P is of a product structure $B\times F$ means that it is a trivial fiber bundle with its base space B and fiber F. In addition, the projective map $\pi: P\to B$ and its inverse $\pi^{-1}: B\to P$ are both continuous. Let P be represented by a pair (B,ζ), where B is the base space of P and ζ is a height field. This formalism provides a general framework and is well suited to the representation in this paper.

We denote an original solid model and its deformed model by P and $\overline{P}$, respectively. The deformation mapping

$$\begin{aligned}&\sigma: P\longrightarrow\overline{P}\\ &(x_1,x_2,x_3)\longrightarrow(y_1,y_2,y_3)\end{aligned} \tag{3}$$

is defined as a composite mapping $\overline{\zeta}\cdot\psi$, and then

$$\overline{P}=\sigma(P)=\overline{\zeta}(\psi(B)), \tag{4}$$

where B is the base patch of P.

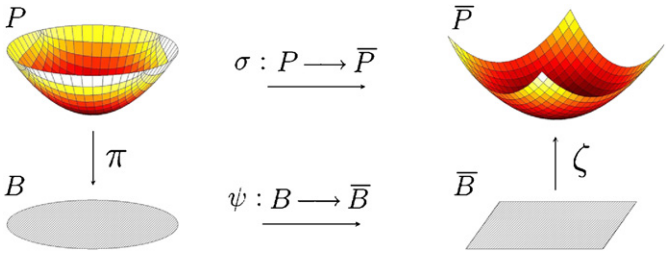

Fig. 2. The deformation procedure.

Precisely, the mapping

$$\psi : B \longrightarrow \overline{B}$$
$$(x_1, x_2) \longrightarrow (u(x_1, x_2), v(x_1, x_2)) \tag{5}$$

between the base patch B and another pre-defined patch $\overline{B}$ depends on a desired deformation. Furthermore, the mapping

$$\overline{\zeta} : \overline{B} \longrightarrow \overline{P}$$
$$(y_1, y_2) \longrightarrow (y_1, y_2, y_3) \tag{6}$$

is the height field associated with the deformed model $\overline{P}$, where $y_1 = u(x_1, x_2)$, $y_2 = v(x_1, x_2)$ and y_3 is determined by a pre-defined function $\varphi(x_1, x_2, x_3)$.

In brief, we define the transformation from P to $\overline{P}$ as

$$\sigma : P \longrightarrow \overline{P}$$
$$(x_1, x_2, x_3) \longrightarrow (u(x_1, x_2), v(x_1, x_2), \varphi(x_1, x_2, x_3)). \tag{7}$$

The deformation procedure can be shown clearly from Fig. 2.

The shape of an original model can be modified by interactive means, such as changing the base patch and adjusting the height field. Let $\overline{B}$ be the objective base patch, then it provides an essential shape of the deformed model in the horizontal direction. Simultaneously, we adopt a section function $\varphi(x_1, x_2, x_3)$ to adjust the shape of the model in the vertical direction.

As mentioned above, we defined the base patch as the projection of P on x_1ox_2 plane. Actually, we can generalize the concept of base patch by defining it as the projection of P on arbitrary plane.

For a versatility of the idea of this paper, our method can be applied to virtually any geometric model such as mesh model and parametric model since the deformation method adopted in this paper is independent of the type of the geometric model. Indeed, the deformation method of the paper can be also used to the field of modeling from some simple primitives. In addition, one can easily apply the method of this paper to a local region of a given model and obtain a local deformation of the model.

5. Base patch mapping

In this section, we consider to construct the base patch mapping by the conformal mapping.

5.1. Schwarz–Christoffel mapping

For a given region with polygonal boundary, a general method of constructing the conformal mapping is offered by Schwarz–Christoffel transformations.

Theorem 1 (*Henrici [23]*). *Suppose a polygon Δ that has complex vertices (possibly infinite) $w_1, w_2, \ldots, w_n$, given in counter-clockwise order. To each vertex w_k $(k = 1, 2, \ldots, n)$ corresponding to an interior turning angle $\alpha_k\pi$ $(k = 1, 2, \ldots, n)$, where $0 < \alpha_k < 2$. Then every function which maps unit disk conformally onto the interior of Δ and satisfies $f(0) = a$ can be expressed in the form*

$$f(z) = a + c\int_0^z \prod_{k=1}^{n}\left(1 - \frac{z}{z_k}\right)^{\alpha_k - 1} \mathrm{d}z, \tag{8}$$

where c is a suitable complex constant, z_k are the pre-vertices of w_k and $|z_k| = 1$ $(k = 1, 2, \ldots, n)$. The map f may be made unique by requiring that $f'(0) = c$ be positive, or by prescribing the position of one pre-vertex z_k.

We denote the map $f(z)$ as a disk-map. A map between two polygons can be obtained by using a composite map which consists of one forward and one inverse disk-map.

We regard the pre-vertices z_k $(k = 1, 2, \ldots, n)$ in (8) as the *parameters* of the Schwarz–Christoffel mapping function. The Schwarz–Christoffel formula is mathematically appealing, but problematic in practice. The main practical difficulty with the formula (8) is that except in special cases, the pre-vertices z_k $(k = 1, 2, \ldots, n)$ cannot be computed analytically. This is the Schwarz–Christoffel parameter problem [24], and its solution is the key problem in any Schwarz–Christoffel map. Once the parameter problem is solved, the multiplicative constant c can be found and the Schwarz–Christoffel formula is an explicit representation of the mapping function f. Though the Schwarz–Christoffel parameter problem cannot be computed analytically, its solution can be numerically solved by the Schwarz–Christoffel toolbox [25] in MATLAB, which is well suited for the interactive computation of Schwarz–Christoffel mappings.

5.2. Generalized Schwarz–Christoffel formula

Suppose a solid model P has serial cross sections B_j at the vertical height h_j $(j = 1, 2, \ldots, m)$. B_j is a simply connected domain and bounded by a polygon Δ_j with complex vertices $w_1^j, w_2^j, \ldots, w_{n_j}^j$, and each vertex w_k^j is corresponding to an interior turning angle $\alpha_k^j\pi$, where $0 < \alpha_k^j < 2$ $(k = 1, 2, \ldots, n_j)$. By Theorem 1, the function which maps unit disk conformally onto B_j can be expressed in the form

$$f_j(z) = a_j + c_j\int_0^z \prod_{k=1}^{n_j}\left(1 - \frac{z}{z_k^j}\right)^{\alpha_k^j - 1} \mathrm{d}z, \tag{9}$$

where a_j and c_j are suitable complex constants, z_k^j are the pre-vertices of w_k^j and $|z_k^j| = 1$ $(j = 1, 2, \ldots, m)$. Then the following piecewise function:

$$f = \begin{cases} f_1, & x_3 = h_1, \\ \vdots & \\ f_j, & x_3 = h_j, \\ \vdots & \\ f_m, & x_3 = h_m \end{cases} \tag{10}$$

maps a cylinder to P in a hierarchical conformal manner, where f_j $(j = 1, 2, \ldots, m)$ is defined in (9). In application, it is desired that a deformed model can be determined by some given patches in the key positions and the number of the patches should be as small as possible.

Definition 2. Two polygon patches B_1 and B_2 are similar if all the corresponding interior angles of them are equal and all the corresponding edges are proportionate (i.e., $B_2 = a + cB_1$, where a and c are two complex constants).

Lemma 2. *Let B_1 and B_2 be two similar polygon patches, f_1 and f_2 be two Schwarz–Christoffel mappings which map unit disk conformally onto B_1 and B_2, respectively. Then f_1 and f_2 have same parameters.*

Proof. The complex constants a and c in formula (8) just determine the position and the size of the polygon [21]. Therefore, if two patches B_1 and B_2 are similar, the Schwarz–Christoffel mapping functions f_1 and f_2 associated with them are only different from the complex constants a and c. In other words, f_1 and f_2 have same parameters. □

Lemma 3. *Let B_1 and B_2 be two similar polygon patches, and the functions which map unit disk D conformally onto B_1 and B_2, respectively, be*

$$f_1(z) = a_1 + c_1 \int_0^z \prod_{k=1}^{n} \left(1 - \frac{z}{z_k}\right)^{\alpha_k - 1} \mathrm{d}z,$$

$$f_2(z) = a_2 + c_2 \int_0^z \prod_{k=1}^{n} \left(1 - \frac{z}{z_k}\right)^{\alpha_k - 1} \mathrm{d}z.$$

Let $B = (1-t)\cdot B_1 + t \cdot B_2$, where t is a real constant, then the function which maps unit disk conformally onto B can be expressed in the form

$$f(z) = a + c \int_0^z \prod_{k=1}^{n} \left(1 - \frac{z}{z_k}\right)^{\alpha_k - 1} \mathrm{d}z, \tag{11}$$

where $a = (1-t)\cdot a_1 + t \cdot a_2$ and $c = (1-t)\cdot c_1 + t \cdot c_2$.

Proof. Apparently B is similar to B_1 and B_2, with Lemma 2, the Schwarz–Christoffel mapping f associated with B have same parameters with f_1 and f_2. We can express f as

$$f(z) = a + c \int_0^z \prod_{k=1}^{n} \left(1 - \frac{z}{z_k}\right)^{\alpha_k - 1} \mathrm{d}z,$$

where a and c are two complex constants. Since $B = (1-t)\cdot B_1 + t \cdot B_2$, then

$$a = (1-t)\cdot a_1 + t \cdot a_2, \quad c = (1-t)\cdot c_1 + t \cdot c_2.$$

Combining the results presented above and the classic interpolation theory, we can get a technique that conformally maps a cylinder to a solid of rotation. In the vertical direction, we define a set of basis functions $\phi_j(h)$ over the interval $[h_1, h_m]$ with interior joints $h_2, h_3, \ldots, h_{m-1}$, which have the following properties:

$$\phi_i(h_j) = \delta_{ij} = \begin{cases} 1, & i = j, \\ 0, & i \neq j, \end{cases} \quad i,j = 1,2,\ldots,m. \tag{12}$$

Furthermore, we define serial similar polygon patches $B_1, B_2, \ldots, B_m$ in parallel with the horizontal plane. With Lemma 3, we can get the following theorem.

Theorem 4. *For a cylinder $P = \{(x_1,x_2,x_3) | x_1^2 + x_2^2 = 1, x_3 \in [t_1, t_m]\}$, denote $P = D \times H$, where $D = \{(x_1,x_2) | x_1^2 + x_2^2 = 1\}$ and $H = \{x_3 | x_3 \in [t_1, t_m]\}$. Suppose a solid of rotation $\overline{P}$ has cross sections B_j at the vertical height h_j $(j = 1,2,\ldots,m)$. Then the function which maps P to $\overline{P}$ in a hierarchical conformal manner can be expressed in the form*

$$F(z;h) = a(h) + c(h) \int_0^z \prod_{k=1}^{n} \left(1 - \frac{z}{z_k}\right)^{\alpha_k - 1} \mathrm{d}z, \tag{13}$$

where $z = x_1 + \mathrm{i}x_2 \in D$, $h \in H$, $\phi_j(h)$ are the basis functions stated in (12), $a(h) = \sum_{j=1}^{m} \phi_j(h) a_j$ and $c(h) = \sum_{j=1}^{m} \phi_j(h) c_j$.

Proof. Based on the properties of $\phi_j(h)$, we have

$$F(z;h_j) = f_j(z) = a_j + c_j \int_0^z \prod_{k=1}^{n} \left(1 - \frac{z}{z_k}\right)^{\alpha_k - 1} \mathrm{d}z,$$

$j = 1,2,\ldots,m.$

Since $f_j(z)$ maps unit disk conformally onto B_j, $F(z;h)$ maps the cross section of P conformally onto the cross section of $\overline{P}$ at the vertical height h_j $(j = 1,2,\ldots,m)$. Furthermore, $\forall h \in H$, we denote $B = \sum_{j=1}^{m} \phi_j(h) B_j$. It is evident that B is a cross section of $\overline{P}$ and is similar to B_j $(j = 1,2,\ldots,m)$. With Lemma 3, we can see $F(z;h)$ maps unit disk conformally onto B. Therefore, $F(z;h)$ maps P to $\overline{P}$ in a hierarchical conformal manner. □

As aforementioned, the mapping function defined in (13) can be used to map a cylinder into a solid of rotation in a layered conformal manner. We call (13) a generalized Schwarz–Christoffel formula.

5.3. Other numerical methods for conformal mapping

Circle packing method was introduced in [26]. A circle packing is a configuration of circles with a specified pattern of tangencies [27]. Thurston conjectured in 1985 [28] that maps between circle packing could be used in the approximation of classical conformal mappings. His conjecture was confirmed by Rodin and Sullivan [29]. Collins and Stephenson [30] have implemented these ideas in their software CirclePack. However, on the more practical side, for those involved in numerical conformal mapping circle packing may appear to be a disappointment: the packing process turns out to be rather slow, data sets are bulky, and the process of laying out the packing itself introduces additional error. Circle packing certainly cannot compete with the classical numerical methods for speed and accuracy [31].

If the base patch B is a domain with smooth bounding ∂B, there are some other methods for numerical evaluation of a conformal mapping from B to unit disk, such as the Szegö method [32], Symm's integral equation method [33], and the Fornberg method [34], etc. Here we do not review them in detail since the limit of this paper.

6. Properties of the deformation method

Jacobian matrices are generally used to compute the transformation of fundamental geometric properties. For C^k $(k \geqslant 1)$ 1–1 mapping

$$f(x_1,\ldots,x_n) = [y_1(x_1,\ldots,x_n),\ldots,y_m(x_1,\ldots,x_n)],$$

the (i,j) element of Jacobian matrix J is $\partial y_i/\partial x_j$, and $\mathrm{d}f = J\,\mathrm{d}X$, where $X = [x_1, x_2, \ldots, x_n]$.

6.1. Topological properties

The Jacobian matrix of the transformation associated with the deformation σ in (7) is

$$J_\sigma = \begin{pmatrix} \frac{\partial u}{\partial x_1} & \frac{\partial u}{\partial x_2} & 0 \\ \frac{\partial v}{\partial x_1} & \frac{\partial v}{\partial x_2} & 0 \\ \varphi'_{x_1} & \varphi'_{x_2} & \varphi'_{x_3} \end{pmatrix}, \tag{14}$$

where $\partial u/\partial x_1, \partial u/\partial x_2, \partial v/\partial x_1, \partial v/\partial x_2$ satisfy the *Cauchy–Riemann condition* stated in (1).

Theorem 5. *For the deformation stated in* (7)*, the deformation is continuous, not self-intersection, and topologically consistent, if and only if $\varphi'_{x_3} > 0$.*

Proof. The determinant of the Jacobian matrix J_σ in (14) is

$$|J_\sigma| = \varphi'_{x_3}\left(\frac{\partial u}{\partial x_1}\cdot\frac{\partial v}{\partial x_2} - \frac{\partial u}{\partial x_2}\cdot\frac{\partial v}{\partial x_1}\right),$$

and $\partial u/\partial x_1$, $\partial u/\partial x_2$, $\partial v/\partial x_1$, $\partial v/\partial x_2$ satisfy the *Cauchy–Riemann condition*, so

$$|J_\sigma| = \varphi'_{x_3}\left[\left(\frac{\partial u}{\partial x_1}\right)^2 + \left(\frac{\partial v}{\partial x_1}\right)^2\right].$$

However, due to the request of conformality $u_{x_1} + iv_{x_1} \neq 0$, and $\varphi'_{x_3} > 0$, then $J_\sigma > 0$, which completes the proof. □

The additional remarks of the theorem are as follows. It is worth noticing that when $|J_\sigma| \leqslant 0$, sometimes it is also useful in practice. In detail, when $|J_\sigma| = 0$, which means that $(\partial u/\partial x_1)^2 + (\partial v/\partial x_1)^2 = 0$ or $\varphi'_{x_3} = 0$, a deformation from a smooth model to a model with edges could be obtained if $(\partial u/\partial x_1)^2 + (\partial v/\partial x_1)^2 = 0$, and a segment of an original model may be pushed down on a special surface if $\varphi'_{x_3} = 0$. When $|J_\sigma| < 0$, that is $\varphi'_{x_3} < 0$, a dimple may be generated on a deformed solid.

6.2. Geometric properties

In computer graphics, surface tangent and normal vector of a solid model are two important geometric quantities—the former for delineating and constructing the local geometry, and the latter for obtaining surface orientation and lighting information [4]. Hereby, we present transformation rules for these quantities associated with the deformation.

For convenience, we denote the surface of a solid model by parametric form $P(s,t) = (x_1(s,t), x_2(s,t), x_3(s,t))$. By chain rule, we have

$$\frac{\partial \overline{P}}{\partial s} = J_\sigma \frac{\partial P}{\partial s} \quad \text{and} \quad \frac{\partial \overline{P}}{\partial t} = J_\sigma \frac{\partial P}{\partial t}, \tag{15}$$

where J_σ is the Jacobian matrix. Since any vector tangent to P is a linear combination of the partial derivatives of $P(s,t)$, the transformation rule for the tangent vectors is

$$T_1 = J_\sigma T, \tag{16}$$

where T are the tangent vectors of an original model's surface and T_1 are the tangent vectors of its deformed model's surface.

At any points of the surface, we have $N \cdot T = N^{\mathrm{T}} T = 0$. Since $N^{\mathrm{T}} T = N^{\mathrm{T}}(J_\sigma^{-1} J_\sigma) T = (N^{\mathrm{T}} J_\sigma^{-1}) T_1 = 0$ and $N_1^{\mathrm{T}} T_1 = 0$, then $N_1^{\mathrm{T}} T_1 = (N^{\mathrm{T}} J_\sigma^{-1}) T_1$, so the transformation rule for the normal vectors is

$$N_1 = (J_\sigma^{-1})^{\mathrm{T}} N, \tag{17}$$

where N are the normal vectors of an original model's surface and N_1 are the normal vectors of its deformed model's surface.

With Eq. (2), it is evident that

$$\begin{pmatrix} \frac{\partial u}{\partial x_1} & \frac{\partial u}{\partial x_2} \\ \frac{\partial v}{\partial x_1} & \frac{\partial v}{\partial x_2} \end{pmatrix} = \begin{pmatrix} \rho\cos\theta & -\rho\sin\theta \\ \rho\sin\theta & \rho\cos\theta \end{pmatrix}, \tag{18}$$

where $\rho = \rho(x_1, x_2)$ is a scalar function and $\theta = \theta(x_1, x_2)$ is a rotation function. Therefore, J_σ can be expressed in the form

$$J_\sigma = S(P)R(P), \tag{19}$$

where $S(P)$ is a scale matrix defined as

$$S(P) = \begin{pmatrix} \rho(x_1,x_2) & 0 & 0 \\ 0 & \rho(x_1,x_2) & 0 \\ \varphi'_{x_1} & \varphi'_{x_2} & \varphi'_{x_3} \end{pmatrix}, \tag{20}$$

and $R(P)$ is a rotation matrix defined as

$$R(P) = \begin{pmatrix} \cos\theta(x_1,x_2) & -\sin\theta(x_1,x_2) & 0 \\ \sin\theta(x_1,x_2) & \cos\theta(x_1,x_2) & 0 \\ 0 & 0 & 1 \end{pmatrix}. \tag{21}$$

Obviously, the angle between any two tangent vectors is holding after deformation, and an infinitesimal curved triangle is transformed into a similar one. Thus, the scheme is locally equiareal. In other words, the deformation preserves the rigid-body properties of a model locally.

6.3. Volume-preserving property

Suppose that the volume of any differential element of a solid model is $\mathrm{d}x_1\,\mathrm{d}x_2\,\mathrm{d}x_3$, then after deformation, the volume becomes $J_\sigma \cdot \mathrm{d}x_1\,\mathrm{d}x_2\,\mathrm{d}x_3$. The volume of the entire deformed solid is simply the triple integral of this differential volume over the volume enclosed by the undeformed surface [6].

Theorem 6. *For the deformation stated in* (7)*, the Jacobian matrix of it is expressed in* (19)*. If* $\varphi'_{x_3} \cdot \rho^2(x_1, x_2) \equiv 1$*, the deformation is volume-preserving.*

Proof. As shown in (19)–(21), the determinant of the Jacobian matrix J_σ is

$$|J_\sigma| = \varphi'_{x_3} \cdot \rho^2(x_1, x_2).$$

Since $\varphi'_{x_3} \cdot \rho^2(x_1, x_2) \equiv 1$, then $|J_\sigma| \equiv 1$. □

7. Implementation and experiments

In this section, we expound our deformation procedure with two algorithms and present some numerical examples to make out our method clearly.

Algorithm 1. Deformation in general form.

Input: A solid model P, and a polygon patch $\overline{B}$.
Output: A target solid model $\overline{P}$.
1. Project P on the horizontal plane. The base patch B of P is the projection.
2. Deform P by conformally mapping the base patch B onto the pre-defined polygon patch $\overline{B}$.
3. Further adjust the height field of P, then generate the target model $\overline{P}$.

In Algorithm 1, the crucial step is step 2, which is the Schwarz–Christoffel mapping problem. As aforementioned in Section 4.1, we solve it by the Schwarz–Christoffel toolbox [25]. In step 3, the height field of P is adjusted by a pre-defined function.

Algorithm 2. Deformation in hierarchy.

Input: A solid model P, a set of polygon patches $\overline{B_1}, \overline{B_2}, \ldots, \overline{B_m}$, and a set of interpolation basis functions ϕ_j $(j = 1, 2, \ldots, m)$.
Output: A target solid model $\overline{P}$.
1. Sample the given solid model P into a set of cross sections B_j $(j = 1, 2, \ldots, m)$.
2. Deform P by conformally mapping every cross section B_j onto the pre-defined polygon patch $\overline{B_j}$ $(j = 1, 2, \ldots, m)$.
3. Move $\overline{B_j}$ $(j = 1, 2, \ldots, m)$ to a bottom-up hierarchy.
4. Generate the target solid model $\overline{P}$ by interpolating $\overline{B_j}$ with the pre-defined interpolation basis functions ϕ_j $(j = 1, 2, \ldots, m)$.

In Algorithm 2, the interpolation basis functions ϕ_j ($j = 1, 2, \ldots, m$) which satisfy the conditions in Eq. (12) are pre-defined by according to user's desired geometric requirements.

7.1. Experiments

The techniques presented in this paper have been implemented and tested on several models with genus zero. Four models—the human face model in Fig. 3, the teapot model in Fig. 4, the David head model in Fig. 5 and the sphere model in Fig. 6, are tested based on Algorithm 1. Meanwhile, the cylinder model in Fig. 8 is tested based on Algorithm 2.

Precisely, for Fig. 3, the original human face (a_1) is deformed to (a_2) and (a_3) by using the conformal mappings $f(z) = e^{-iz}$ and $f(z) = e^{iz}$, respectively, where $z = x_1 + ix_2$ and i is the imaginary unit. For Fig. 4, we implement deformation with a teapot. From the first row to the third row of Fig. 4, the models have disk base patch, square base patch and hexagon base patch, respectively. And the models in each columns of Fig. 4 have the same height fields. In column (b_1), the models' height field are unchanged. The height field functions associated with the models in column $(b_2)-(b_6)$ are listed in Table 2. Fig. 5 is an example of David head deformation. Head (c_1) is the original model, (c_2) is a deformation of (c_1) by conformally mapping its base patch into a triangular domain and maintaining its height field unchanged, and (c_3) is a deformation by conformally mapping its base patch into a rectangular domain and changing its height field. For Fig. 6, some deformation models are yielded from a sphere. The sphere deformation includes conformal mapping its base patches in the horizontal direction and adjusting the height field in the vertical direction. Precisely, we first deform the sphere into the models in the second row of Fig. 6 by conformally changing its base patch from a disk domain to a square domain, a regular hexagon domain, and etc.; then we adjust the height field of the models in the second row to yield the models in the third row of Fig. 6. Fig. 8 illustrates the deformation from a cylinder to two chesses in a hierarchical divisible conformal manner.

Five sectional conformal mappings associated with the sphere deformation—the mappings on disk to square, hexagon, pentagram, spindle and plum blossom, respectively, are illustrated in Fig. 7. As shown in Fig. 7 in which the conformal property, the local orthogonality of the interior of the regions, is preserved. In addition, the parameters of the Schwarz–Christoffel formula of these mappings are listed in Tables 3–7.

As a matter of fact, in the implement of the deformation, we just need to know the boundary of the base patch of an objective model to determine its base patch mapping and then we can further adjust the shape of the model by changing its height field.

7.2. Complexity analysis

In practice, the crucial step in the implement of our method is the construction of base patch mapping. For patches with polygon boundaries, we use Schwarz–Christoffel formula to construct the conformal mappings between them. The complexity for the evaluation of the integral in the Schwarz–Christoffel formula is $O(N)$ and the evaluation of the parameters in the formula is $O(N^3)$, where N is the number of polygon vertices. It looks that it is not efficient for mapping between complicated regions. In fact, we first select the region of the original model to be deformed and use as few vertices as possible to determine the region's boundary. The implement is efficient because the number of the vertices is always very small.

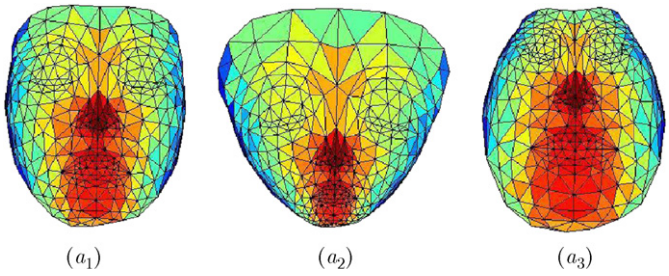

Fig. 3. Human face deformation.

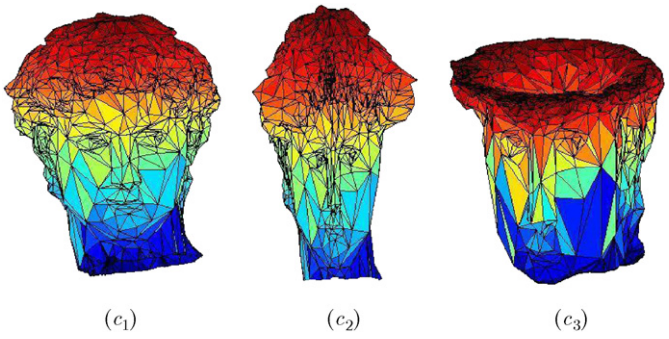

Fig. 5. David head deformation.

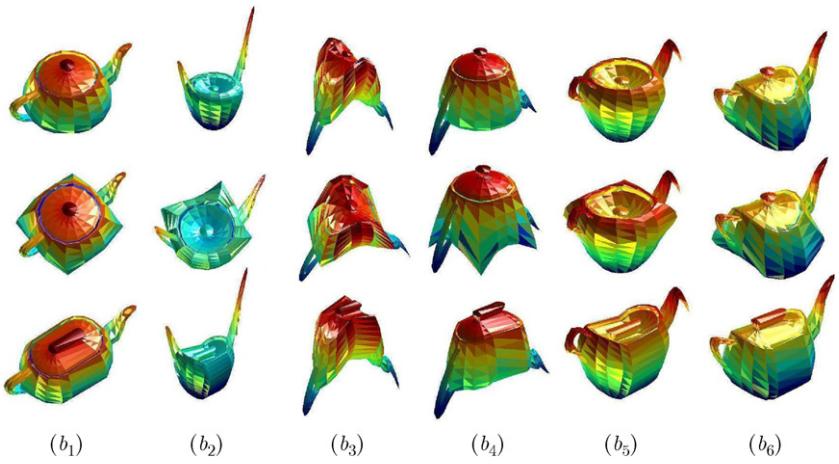

Fig. 4. Teapot deformation.

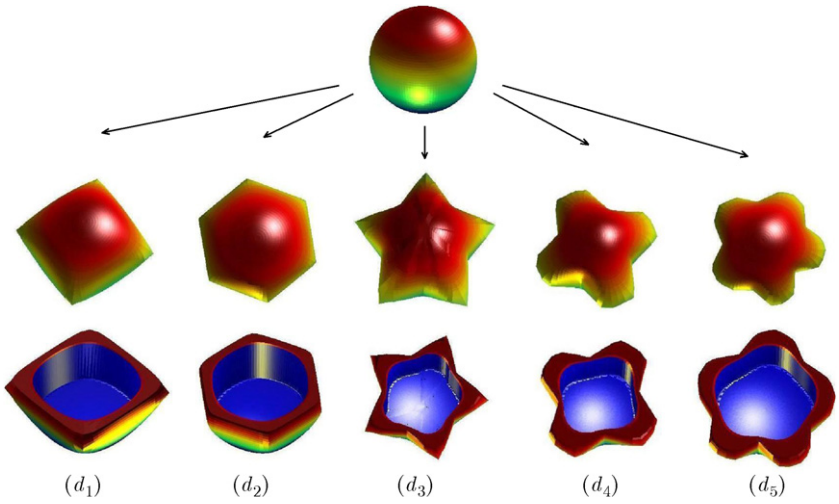

Fig. 6. Sphere deformation.

Table 1
Time requirements for the examples

Model	Verts	Tris	Eval/s
Human face (Fig. 3)	299	562	0.0832
David head (Fig. 5)	1512	2924	2.1853
Sphere (Fig. 6)	7082	14160	3.0293
Teapot (Fig. 4)	530	1024	5.2991
Cylinder (Fig. 8)	4762	9520	3.4313

Table 2
The height fields of the models in column $(d2)-(d6)$ of Fig. 8

$d2$	$d3$	$d4$	$d5$	$d6$
x^2+y^2+z	$-x^2+y^2+z$	$\cos(x^2+y^2)+z$	$\sin(x^2+y^2)+z$	$\frac{x^2}{4}-\frac{y^2}{2.25}+z$

All the experiments in this paper are implemented on a Intel Pentium 4 2.60 GHz computer with 512 MB of RAM. Time requirements for examples given in the paper are listed in Table 1. Our technique is currently implemented to triangular mesh models. *Verts* and *Tris* in Table 1 denote the number of the vertices and facets of the model. In every examples we select the average time. In addition, it need to be stressed that the deformation method in the paper is not limited to triangular mesh model, and it can be applied to other models such as quad mesh model, parametric model, etc.

8. Conclusion

A novel layered deformation method via conformal mapping is presented in this paper. The method is convenient and intuitive to deform both the surface and the volume of a 3D solid model.

Actually, the construction of the base patch mapping is a key step in our method. To construct the map, we specify a polygon that determines the target domain and invoke a map constructor in Schwarz–Christoffel toolbox [25]. The constructor's main task is to find the correct values of the pre-vertices z_k in formula (8). The conformal center $a(a=f(0))$ and the constant $c(c=f'(0))$ in formula (8) can be set by the map constructor. On the other hand, there may be an inaccurate map to be constructed when the specified pre-vertices which are not computed from the map constructor are used, since the pre-vertices may be not compatible with the given polygon. Moreover, in our method the height field and the similar polygons are approximately determined by interpolation according to the target of deformation as user's requirements. Because of these, the method of the paper need to be further improved in the aspects such as the precise control of pre-vertices and the limitations of the specification of the height field and the employment of similar polygons in the hierarchical scheme to general cases.

Furthermore, our main attention of the paper is to consider the layered conformal deformation to a solid model with genus zero. For a solid model with genus greater than zero, generally, holes in domains lead to two difficulties in model's deformation by conforming mapping. Firstly, for conformal mapping between two regions in the complex plane, both regions must have the same connectivity. Secondly, Riemann's mapping theorem no longer holds [21]. It can be shown in a fairly straightforward manner that it is not always possible to map one doubly connected region onto another. In fact, the only conformal map of one annulus onto another (assuming, without loss of generality, that their centers are at the origin) is a linear transformation. As a direct consequence, all annuli that are the image of a given doubly connected geometrically similar, and therefore have the same ratio of inner and outer ratio. This ratio is known as the modulus of the doubly connected domain. Furthermore, since any doubly connected domains can be mapped onto an annulus, it also follows that two doubly connected domains cannot be conformally mapped onto each other unless they have the same modulus.

Surface Ricci flow was first introduced by Hamilton [35] and has been applied for the proof of Poincare conjecture. Ricci flow refers to conformally deform the Riemann metric of a surface by its Gaussian curvature, such that the curvature evolved according to a heat diffusion process [36]. Ricci flow can handle arbitrary topologies and find arbitrary conformal mappings. The connection between circle packing and smooth Ricci flow was discovered in [37]. Circle packing only considers combinatorial structures but not geometric information. The discrete Ricci flow method was introduced in [38,39], which incorporate geometric information and has been applied to compute the geometric structures of surfaces [40,41].

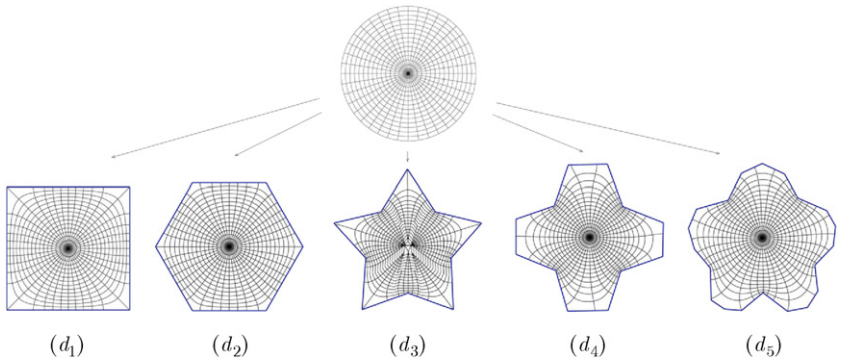

Fig. 7. Base patch conformal mappings (conformal sectional mappings) corresponding to the sphere deformation; map a disk domain into domains (d_1)–(d_5): the local orthogonality of the curves in the disk is preserved after deformation.

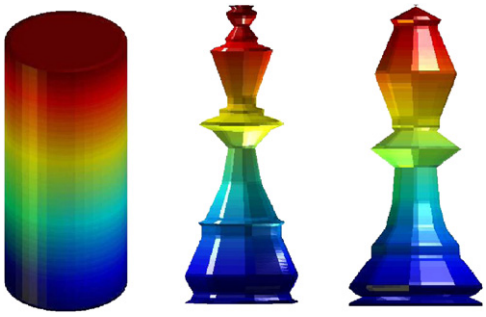

Fig. 8. Cylinder deformation.

Table 3
The parameters of the mapping between a disk domain and a square domain

Vertex	Alpha	Pre-vertex	Arg/pi
1.00000 + 1.00000i	0.50000	0.70711 + 0.70711i	0.250000000000
−1.00000 + 1.00000i	0.50000	−0.70711 + 0.70711i	0.750000000000
−1.00000 − 1.00000i	0.50000	−0.70711 − 0.70711i	1.250000000000
1.00000 − 1.00000i	0.50000	0.70711 − 0.70711i	1.750000000000

$c = 1.0787027 + 0i$, conformal center at $0.0000 + 0.0000i$.

Table 4
The parameters of the mapping between a disk domain and a regular hexagon domain

Vertex	Alpha	Pre-vertex	Arg/pi
0.50000 + 0.86600i	0.66667	0.50002 + 0.86601i	0.333324776669
−0.50000 + 0.86600i	0.66667	−0.50002 + 0.86601i	0.666675222417
−1.00000 + 0.00000i	0.66666	−1.00000 + 0.00000i	0.999999999365
−0.50000 − 0.86600i	0.66667	−0.50002 − 0.86601i	1.333324776437
0.50000 − 0.86600i	0.66667	0.50002 − 0.86601i	1.666675222555
1.00000 + 0.00000i	0.66666	1.00000 + 0.00000i	2.000000000000

$c = 0.89852992 + 1.2026493e - 009i$, conformal center at $0.0000 + 0.0000i$.

For the deformation of solid models with arbitrary topological structures, we need to proceed with efforts based on the discrete Ricci flow theory or other theories such that the deformation method of this paper valid for any multiply connected objective. Fig. 9 shows the deformation associated with a torus based on our method and the boolean operator theory. Precisely, we conformally map both the outer disk and the inner disk to the

Table 5
The parameters of the mapping between a disk domain and a five-stars domain

Vertex	Alpha	Pre-vertex	Arg/pi
0.95100 + 0.30910i	0.35002	0.95100 + 0.30910i	0.100030688334
0.35880 + 0.45430i	1.23832	0.58780 + 0.80900i	0.299993022552
0.00000 + 1.00000i	0.36300	0.00000 + 1.00000i	0.500000000000
−0.34120 + 0.45430i	1.24773	−0.58780 + 0.80900i	0.700006977448
−0.95100 + 0.30910i	0.34096	−0.95100 + 0.30910i	0.899969311666
−0.54120 − 0.14570i	1.25577	−0.95100 − 0.30910i	1.100030688334
−0.58780 − 0.80900i	0.36838	−0.58780 − 0.80900i	1.299993022552
0.00880 − 0.59570i	1.22165	0.00000 − 1.00000i	1.500000000000
0.58780 − 0.80900i	0.37374	0.58780 − 0.80900i	1.700006977448
0.55880 − 0.14570i	1.24042	0.95100 − 0.30910i	1.899969311666

$c = 0.42981899 - 0.13972703i$, conformal center at $0.0000 + 0.0000i$.

Table 6
The parameters of the mapping between a disk domain and a spindle domain

Vertex	Alpha	Pre-vertex	Arg/pi
−0.30000 − 1.00000i	0.58433	0.79918 + 0.60110i	0.205269178666
0.25000 − 0.99000i	0.60459	0.66689 + 0.74516i	0.267625915377
0.42000 − 0.46000i	1.29379	0.06417 + 0.99794i	0.479561524841
0.99000 − 0.26000i	0.61433	−0.62729 + 0.77879i	0.715835797596
1.00000 + 0.20000i	0.61420	−0.73424 + 0.67889i	0.762459323204
0.45000 + 0.42000i	1.26652	−0.99974 + 0.02261i	0.992800818328
0.24000 + 0.99000i	0.60636	−0.73436 − 0.67876i	1.237483346943
−0.29000 + 0.98000i	0.61188	−0.58382 − 0.81188i	1.301556922479
−0.48000 + 0.43000i	1.28805	0.07960 − 0.99683i	1.525363480531
−1.00000 + 0.25000i	0.60607	0.65009 − 0.75986i	1.725268872496
−1.00000 − 0.23000i	0.62315	0.76496 − 0.64408i	1.777241575753
−0.46000 − 0.45000i	1.28674	1.00000 + 0.00000i	2.000000000000

$c = -0.53622672 - 0.52873955i$, conformal center at $0.0000 + 0.0000i$.

objective polygons and use the boolean subtraction to get the expected result.

Generally, the solid models considered in computer graphics are differential manifolds and have local direct product structures at least. For a model which is not of a global direct structure, we can treat it as a general fiber bundle over the base space and adapt our method for it by conformally deforming its base space and properly adjusting its fiber. Taking Möbius strip as an example, whose base space is a unit circle, we apply our method to it by conformally transforming its circular base space into a square base space and making its fiber unchanged. The deformation associated with the Möbius strip is illustrated in Fig. 10.

Table 7
The parameters of the mapping between a disk domain and a plum blossom domain

Vertex	Alpha	Pre-vertex	Arg/pi
$0.01000 - 0.74000i$	1.42643	$0.89667 + 0.44271i$	0.145981513318
$0.34000 - 0.99000i$	0.73534	$0.58829 + 0.80865i$	0.299801959090
$0.61000 - 0.94000i$	0.73868	$0.51403 + 0.85777i$	0.328152657145
$0.75000 - 0.72000i$	0.78338	$0.43434 + 0.90075i$	0.356979956964
$0.71000 - 0.37000i$	1.27998	$0.08386 + 0.99648i$	0.473273817487
$0.96000 - 0.11000i$	0.79146	$-0.36021 + 0.93287i$	0.617293845051
$0.99000 + 0.16000i$	0.79953	$-0.50420 + 0.86358i$	0.668213974467
$0.87000 + 0.37000i$	0.79610	$-0.61799 + 0.78619i$	0.712052571755
$0.48000 + 0.54000i$	1.20606	$-0.95232 + 0.30510i$	0.901309637829
$0.30000 + 0.86000i$	0.80208	$-0.97645 - 0.21575i$	1.069218966375
$0.00000 + 1.00000i$	0.72266	$-0.91345 - 0.40695i$	1.133406392393
$-0.28000 + 0.87000i$	0.78594	$-0.82831 - 0.56027i$	1.189304029499
$-0.46000 + 0.51000i$	1.26579	$-0.35607 - 0.93446i$	1.384117021118
$-0.89000 + 0.39000i$	0.71403	$0.23980 - 0.97082i$	1.577081693477
$-1.00000 + 0.13000i$	0.78401	$0.37319 - 0.92775i$	1.621736827867
$-0.92000 - 0.15000i$	0.86505	$0.54444 - 0.83880i$	1.683257117068
$-0.70000 - 0.41000i$	1.21613	$0.85600 - 0.51698i$	1.827055787319
$-0.69000 - 0.84000i$	0.69457	$0.98824 - 0.15291i$	1.951134361337
$-0.51000 - 0.96000i$	0.84044	$0.99625 - 0.08650i$	1.972431080937
$-0.28000 - 0.98000i$	0.75233	$1.00000 + 0.00000i$	2.000000000000

$c = -0.36319196 - 0.7659013i$, conformal center at $0.0000 + 0.0000i$.

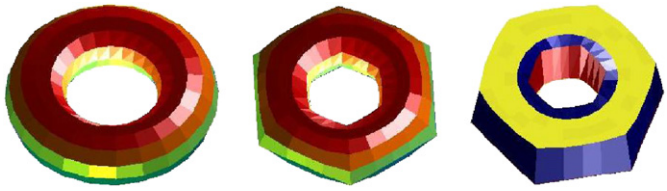

Fig. 9. Torus deformation.

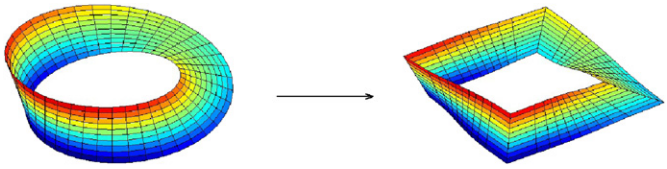

Fig. 10. Möbius strip deformation.

Acknowledgments

The authors would like to express their thanks to the reviewers for their valuable comments and suggestions that significantly contributed to the improvement of this paper. Many thanks are given to Doctor Meng Zhaoliang for his constructive recommendations that helped us to finish the work.

References

[1] Bechmann D, Bertrand Y, Thery S. Continuous free form deformation. Computer Networks and ISDN Systems 1997;29(14):1715–25.
[2] Bechmann D. Space deformation models survey. Computers & Graphics 1994;18(4):571–86.
[3] Watt A, Watt M. Advanced animation and rendering technique. Reading, MA: Addison-Wesley; 1992.
[4] Barr AH. Global and local deformation of solid primitives. Computer & Graphics 1984;17(3):21–30.
[5] Borrel P, Bechmann D. Deformation of *N*-dimensional objects. International Journal of Computational Geometry and Applications 1991;1(4):427–53.
[6] Sederberg TW, Parry R. Free-form deformation of solid geometric models. In: SIGGRAPH 86, ACM computer graphics, vol. 20(4), 1986. p. 151–60.
[7] Coquillart S. Externed free-form deformation: a sculpturing tool for 3D geometric modeling. In: SIGGRAPH 90, ACM computer graphics, vol. 24(4), 1990. p. 187–96.
[8] MacCracken R, Ki J. Free-form deformations with latices of arbitrary topology. In: SIGGRAPH 96, 1996. p. 181–8.
[9] Lazarus F, Coquillart S, Jancene P. Axial deformation: an intuitive technique. Compter-Aided Design 1994;26(8):607–13.
[10] Feng JQ, Ma LZ, Peng QS. A new free-form deformation through the control of parametric surfaces. Computers & Graphics 1996;20(4):531–9.
[11] Alexa M. Differential coordinates for local mesh morphing and deformation. The Visual Computer 2003;19(2):105–14.
[12] Lipman Y, Sorkine O, Cohen-Or D, Levin D, Rossl C, Seidel H-P. Differential coordinates for interactive mesh editing. In: SMI 2004: proceedings of the international conference on shape modeling and applications, 2004. p. 181–90.
[13] Lipman Y, Sorkine O, Levin D, Cohen-Or D. Linear rotation-invariant coordinates for meshes. ACM Transactions on Graphics 2005;24(3):479–87.
[14] Sorkine O, Cohen-Or D, Lipman Y, Alexa M, Rossl C, Seidel H-P. Laplacian surface editing. In: Proceedings of the symposium on geometry processing, 2004. p. 175–84.
[15] Zhou K, Huang J, Snyder J, Liu X, Bao H, Guo B, et al. Large mesh deformation using the volumetric graph Laplacian. ACM Transactions on Graphics 2005;24(3):496–503.
[16] Ju T, Schaefer S, Warren J. Mean value coordinates for closed triangular meshes. ACM Transactions on Graphics 2005;24(3):561–6.
[17] Pushkar J, Mark M, Tony DR, Brian G, Tom S. Harmonic coordinates for character articulation. In: SIGGRAPH '07: ACM transactions on graphics, vol. 26(3), 2007. p. 71–80.
[18] Alexa M. Mesh editing based on discrete Laplace and Poisson models. In: SIGGRAPH '06: ACM SIGGRAPH 2006 courses, 2006. p. 51–9.
[19] Zayer R, Rossl C, Karni Z, Seidel H-P. Harmonic guidance for surface deformation. Computer Graphics Forum 2005;24(3):601–9.
[20] Huang J, Chen L, Liu X, Bao H. Efficient mesh deformation using tetrahedron control mesh. In: Proceedings of ACM symposium on solid and physical modeling, 2008. p. 241–7.
[21] Nehari Z. Conformal mapping. New York: Dover Publications Inc.; 1952.
[22] Krantz SG. Conformal mappings. American Scientist 1999;87(5):436–45.
[23] Henrici P. Applied and computational complex analysis, vol. 1. New York: Wiley; 1974.
[24] Henrici P. Applied and computational complex analysis, vol. 3. New York: Wiley; 1986.
[25] Driscoll TA. Algorithm 756: A MATLAB toolbox for Schwarz–Christoffel mapping. ACM Transactions on Mathematical Software 1996;22(2):168–86.
[26] Thurston WP. Geometry and topology of three-manifolds. Princeton lecture notes. Princeton, NJ: Princeton University Press; 1976.
[27] Stephenson K. Introduction to circle packing: the theory of discrete analytic functions. Cambridge: Cambridge University Press; 2005.
[28] Thurston WP. The finite Riemann mapping theorem. In: Invited talk, An international symposium at Purdue University on the occasion of the proof of the Bieberbach conjecture, March 1985.
[29] Rodin B, Sullivan D. The convergence of circle packing to the Riemann mapping. Journal of Differential Geometry 1987;26(3):349–60.
[30] Collins C, Stephenson K. A circle packing algorithm. Computational Geometry: Theory and Applications 2003;25:233–56.
[31] Stephenson K. The approximation of conformal structures via circle packing. In: Computational methods and function theory 1997, Proceedings of the third CMFT conference, vol. 11. Singapore: World Scientific; 1999. p. 551–82.
[32] Kerzman N, Trummer MR. Numerical conformal mapping via the Szegö kernel. Journal of Computational and Applied Mathematics 1986;14:111–23.
[33] Symm GT. An integral equation method in conformal mapping. Numerical Mathematics 1966;9:250–8.
[34] Fornberg B. A numerical method for conformal mapping. SIAM Journal on Scientific and Statistical Computing 1980;1:231–50.
[35] Hamilton RS. The Ricci flow on surfaces. Mathematics and General Relativity 1988;71:237–62.
[36] Jin M, Luo F, Gu XF. Computing general geometric structures on surfaces using Ricci flow. Computer-Aided Design 2007;39(8):663–75.
[37] Chow B, Luo F. Combinatorial Ricci flows on surfaces. Journal of Differential Geometry 2003;63(1):97–129.
[38] Jin M, Luo F, Gu XF. Computing surface hyperbolic structure and real projective structure. In: ACM symposium on solid and physics modeling, 2006. p. 105–16.
[39] Gu XF, He Y, Jin M, Luo F, Qin H, Yau S-T. Manifold splines with single extraordinary point. In: ACM symposium on solid and physical modeling, 2007. p. 61–72.
[40] Jin M, Kim J, Gu XF. Discrete surface Ricci flow: theory and applications. In: IMA conference on the mathematics of surfaces. Lecture notes in computer science, vol. 4647. Berlin: Springer; 2007. p. 209–32.
[41] Gu XF, Yau S-T. Computational conformal geometry. Beijing: Higher Education Press; 2008.